RESEARCH PAPER

Harnessing Artificial Intelligence for the Rational Design and Optimization of Chitosan-Tripolyphosphate Nanoparticles Loaded with Curcumin: A Deep Learning and Bayesian Optimization Approach to Oral Bioavailability Enhancement

Monali Chaudhari[1], Tilottama Pankaj Dhake[2], Milind Gajare[3], Diksha Parag Chopade[3], Pravin Gawande[4], Manish Rana[5], Altaf O. Mulani[6*]

[1]*Assistant Professor, VES Institute of Technology,Mumbai, India*
[2]*Assistant Professor, K. J. Somaiya Institute of Technology,Sion, India*
[3]*Assistant Professor, AISSMS Institute of Information Technology, Pune, India*
4Assistant Professor, Vishwakarma Institute of Technology, Pune, India
[5]*Associate Professor, Shah and Anchor Kutchhi College of Engineering, Mumbai, India*
[6]***Professor, SKN Sinhgad College of Engineering, Korti, Pandharpur, India*

ABSTRACT

Curcumin, a phenolic pigment isolated from Curcuma longa, holds well-documented therapeutic relevance across oncology, neurology, and inflammatory disease. Yet its journey from laboratory promise to clinical reality has been repeatedly derailed by an extremely low oral bioavailability that barely exceeds one percent, a consequence of negligible aqueous solubility, fast metabolic conjugation, and limited intestinal permeability. Encapsulating curcumin within chitosan-tripolyphosphate (CS-TPP) nanoparticles prepared through ionic gelation has long been recognised as a viable strategy to surmount these barriers, but identifying the precise combination of chitosan concentration, drug payload, and crosslinker ratio that simultaneously satisfies targets for particle size, colloidal stability, and encapsulation remains a formidable multivariate challenge when addressed through conventional trial-and-error experimentation. The present work therefore embedded artificial intelligence at the centre of the formulation development workflow. A multilayer perceptron (MLP) network trained on 120 systematically generated batches learned the complex, nonlinear landscape connecting three process inputs to four physicochemical outputs with a test-set R^2 of 0.9943 for particle size — markedly better than a Box-Behnken polynomial model applied to the same dataset. Bayesian optimisation with a Gaussian Process surrogate and Expected Improvement acquisition subsequently located the global optimum in 31 guided iterations rather than the eighty-plus experiments a full factorial screen would have demanded. The AI-recommended formulation — 0.30% w/v chitosan, 5.5 mg curcumin, 1:5 TPP ratio — was synthesised and characterised independently. Particle size settled at 182 ± 9 nm, PDI at 0.17 ± 0.02, zeta potential at +33.6 ± 1.7 mV, and encapsulation efficiency at 86.9 ± 2.1%, each within 6% of the model prediction. Release in phosphate-buffered saline followed anomalous (non-Fickian) kinetics with 79.8% cumulative delivery at 24 h. Apparent permeability across Caco-2 monolayers was 3.9-fold higher than that of unformulated curcumin, and cytotoxic potency against HCT-116 colon carcinoma cells improved 5.7-fold. Beyond the formulation outcomes, the study documents a reproducible AI-pharmaceutical template that shortened the optimization timeline by roughly two-thirds relative to conventional design strategies...

Keywords: Artificial intelligence; chitosan nanoparticles; curcumin oral delivery; Bayesian optimization; multilayer perceptron; bioavailability enhancement

How to cite this article: Chaudhari M, Dhake TP, Gajare M, Chopade DP, Gawande P, Rana M, Mulani AO: Harnessing Artificial Intelligence for the Rational Design and Optimization of Chitosan-Tripolyphosphate Nanoparticles Loaded with Curcumin: A Deep Learning and Bayesian Optimization Approach to Oral Bioavailability Enhancement. .Int J Drug Deliv Technol. 2026;16 (3s): 998-1006; DOI: 10.25258/ijddt.16.3s.120

Source of support:. None
Conflict of interest: None

INTRODUCTION

Finding the sweet spot in nanoparticle formulation has always demanded patience. Researchers typically cycle through dozens or hundreds of batches, adjusting one or two variables at a time while measuring particle size, zeta potential, and drug payload on each occasion. Even when a structured statistical design such as Box-Behnken or central composite design replaces pure empiricism, the resulting polynomial models impose a ceiling on predictive fidelity because they cannot capture the steep, asymmetric, and occasionally discontinuous response surfaces that characterize ion-cross-linked polymeric systems. This gap between what the formulation scientist needs to know and what conventional methods can reliably reveal has grown increasingly uncomfortable as the complexity of nanomedicine formulations rises [1].

Artificial intelligence offers a genuinely different philosophy. Rather than fitting a predetermined

**Author for Correspondence: draomulani.vlsi@gmail.com*

mathematical skeleton to the data, machine learning models discover structure bottom-up from observations, giving them the freedom to represent relationships of arbitrary shape. For pharmaceutical nanoparticle development, this matters enormously: the ionotropic gelation of chitosan with tripolyphosphate involves simultaneous proton-transfer equilibria, electrostatic pairing, polymer chain entanglement, and surface adsorption events whose combined effect on particle architecture is highly nonlinear and difficult to capture with second-order polynomial approximations [2].

Curcumin provides an instructive case study in why improved formulation strategies are urgently needed. With roughly 120 clinical trials registered against targets ranging from colorectal cancer to Alzheimer disease, the molecule has attracted more investigational attention than almost any other natural product. Yet every human pharmacokinetic study tells essentially the same story: oral doses of even two grams generate peak plasma concentrations barely above 20 ng/mL, the compound vanishes within hours through hepatic and intestinal glucuronidation, and the downstream tissue concentrations needed for pharmacological effect are never reliably achieved. The root cause is a physicochemical profile BCS Class IV, meaning simultaneously poor solubility and poor permeability that conventional formulation strategies have so far failed to overcome comprehensively [3].

Chitosan nanoparticles have earned genuine enthusiasm in this context for several mechanistically sound reasons. The polycation's adhesive interaction with gastrointestinal mucin prolongs residence at the absorption site; its documented capacity to loosen tight junctions transiently opens the paracellular route; and its own biodegradation generates non-toxic metabolites that the body handles through normal nitrogen pathways. Ionic crosslinking with TPP avoids organic solvents and elevated temperatures, preserving curcumin's photosensitive chromophore. The challenge is that none of these advantages is guaranteed they depend on obtaining nanoparticles within a fairly narrow window of size, charge, and matrix density, and locating that window through experimentation alone is costly [4].

The multilayer perceptron is among the most versatile function approximators available to the formulation scientist. Stacked layers of neurons connected by learnable weights, activated through rectified linear or sigmoid functions, can represent virtually any mapping from inputs to outputs given sufficient training data and appropriate regularisation. Unlike k-nearest-neighbour models that interpolate directly between training points, a trained MLP generalises to new regions of the design space precisely the property needed when formulation constraints prevent full factorial coverage [5].

Bayesian optimisation complements the predictive model by providing a rational strategy for selecting which experiment to run next. The Gaussian Process surrogate maintains a probabilistic estimate of the response surface at every untested point; the acquisition function then trades off between exploiting high-predicted-desirability regions and exploring areas where prediction uncertainty is large. The result is a sequential experimental protocol that converges on the global optimum with remarkable economy of effort, typically requiring far fewer evaluations than grid or random search at comparable confidence levels [6].

Explainability has emerged as an equally important consideration as accuracy. A formulation scientist cannot act on a model that merely outputs a prediction without any indication of why that prediction was made; regulatory reviewers expect mechanistic justification, not just numerical agreement. SHapley Additive exPlanations (SHAP), rooted in cooperative game theory, decompose each prediction into additive contributions from individual input features and have become the de-facto standard for interpreting complex ML models in pharmaceutical sciences [7].

Long short-term memory networks, a recurrent architecture designed to retain information across variable-length sequences, are particularly well suited to modelling drug release profiles inherently sequential data where each measurement depends on the history of preceding dissolution. Hybrid models that combine a mechanistic diffusion backbone with an LSTM residual corrector have demonstrated marked advantages over either pure physics or pure ML approaches for predicting biphasic release from polymeric matrices [8].

This investigation was structured around four interlocking objectives: first, to build and validate an MLP predictive model for CS-TPP nanoparticle properties from a systematically acquired experimental dataset; second, to deploy Bayesian optimization for efficient identification of the global optimum formulation; third, to characterize the resulting nanoparticles and benchmark their performance against conventionally optimized controls; and fourth, to evaluate the AI recommended formulation against biopharmaceutical endpoints intestinal permeability and cancer cell cytotoxicity that carry direct therapeutic relevance. The broader ambition is to demonstrate that AI centered formulation development is not a speculative aspiration but an operationally mature methodology ready for routine pharmaceutical adoption.

2. LITERATURE SURVEY

Early applications of neural networks in pharmaceutical formulation established that biological data, with its inherent measurement noise and limited sample sizes, could nonetheless support useful predictive models. Rowe and Roberts [1] showed that MLP networks outperformed response surface equations for tablet dissolution from granulation parameters, establishing a conceptual precedent that proved generative for the nanoparticle field. Their finding that two hidden layers sufficed to capture the dominant nonlinearities without overfitting became a useful starting heuristic for subsequent investigators.

Moving from solid dosage forms to nanoparticles, Ahmadi and colleagues [2] trained neural networks on PLGA nanoparticle datasets and documented particle size predictions with root mean square errors well below those obtained from quadratic surface models. What distinguished their analysis was the attention paid to why the ANN outperformed the polynomial: careful examination revealed that it was precisely in the regions where two or more factors

jointly deviated from their center points that the polynomial approximation failed most severely, while the neural network maintained its accuracy — strong evidence that the underlying response landscape is genuinely nonlinear rather than merely quadratic.

The statistical foundations of Bayesian optimization for experimental design were adapted for drug discovery by Griffiths and Hernandez-Lobato [3], whose work on constrained molecular optimization demonstrated that Expected Improvement as an acquisition function reliably located global optima within 25 to 50 iterations across chemical spaces orders of magnitude larger than those encountered in nanoparticle formulation. Their analysis also established that the GP surrogate's uncertainty estimates were well-calibrated, meaning that the algorithm's confidence in its recommendations reflected genuine epistemic uncertainty rather than systematic over or under confidence.

Chitosan nanoparticle formulation using a radial basis function network was described by Abbaspour et al. [4], who noted that the RBF architecture's localized response functions gave it an inherent advantage for datasets where extreme formulation conditions produced behaviors qualitatively different from the central design space, a common occurrence in ionic gelation systems where charge balance shifts can trigger particle aggregation at threshold values of TPP concentration.

The physicochemical barriers confronting curcumin were catalogued most systematically by Sharma et al. [5], whose human pharmacokinetic study documented the cascade of metabolic and solubility limitations that together reduce oral bioavailability below 1%. Their data provided the quantitative benchmarks against which any improved formulation strategy must be evaluated, and their identification of glucuronidation as the dominant metabolic pathway suggested that extended intestinal residence achievable through mucoadhesive nanoparticles would reduce presystemic conversion more effectively than absorption enhancement alone.

Graph neural networks applied to curcumin analogue libraries were explored by Li et al. [6], who demonstrated that molecular-level AI and formulation-level AI represent complementary layers of the same bioavailability improvement strategy. While their study focused on identifying structurally modified curcuminoids with inherently better pharmaceutical properties, the authors argued persuasively that even structurally optimized analogues would benefit from encapsulation strategies, pointing toward a future in which molecular AI and formulation AI operate in concert.

Transfer learning as a solution to small dataset constraints was demonstrated by Shen et al. [7], who pre-trained a deep network on 15,000 publicly available nanoparticle records before fine-tuning on 87 chitosan-specific batches. The 23% reduction in prediction error relative to training from scratch is a practically significant finding because it implies that pharmaceutical companies need not each generate their own large proprietary datasets; instead, pre-trained foundation models anchored in public databases can be customized to specific product types with modest additional experimentation.

Explainability in pharmaceutical AI was addressed systematically by Jimenez-Luna et al. [8], who benchmarked multiple XAI methods and found that SHAP produced the most consistent, mechanistically interpretable attributions across a variety of model architectures. Their recommendation that SHAP analysis accompany every pharmaceutical ML model as a minimum interpretability standard has since been echoed in several regulatory guidance documents, underscoring the practical importance of building explainability into formulation AI workflows from the outset.

Hybrid mechanistic-ML modelling of nanoparticle drug release was pioneered by Dahlgren et al. [9], whose LSTM augmented diffusion model captured both the initial burst and the sustained plateau phases of biphasic release profiles with a fidelity that neither pure physics nor pure data-driven approaches could match individually. The key architectural insight was that the mechanistic skeleton constrained the LSTM to physically plausible trajectory shapes, eliminating the implausible oscillations that unconstrained sequence models sometimes generate when extrapolating beyond the training range.

Multi-objective optimization on ANN surrogates was formalized for nanoparticle systems by Rantanen and Khinast [10], who used evolutionary algorithms to generate Pareto fronts that made the trade-off between small particle size and high encapsulation efficiency visible and actionable for formulation scientists. Their conclusion that particles below 150 nm typically cannot exceed 70% encapsulation in chitosan-TPP systems because the polymer matrix at low concentration is simply too sparse to retain hydrophobic cargo at high loading set a realistic expectation boundary that informed the target ranges used in the present study.

The breadth of AI adoption across pharmaceutical development was surveyed by Aliper et al. [11], who documented applications spanning virtual screening, toxicity prediction, clinical trial design, and formulation optimization. Their survey noted that formulation optimization was among the fastest-growing AI application areas in the pharmaceutical sector, driven partly by the relatively modest dataset requirements, hundreds rather than millions of training examples that make pharmaceutical ML more accessible to research groups without industrial-scale data infrastructure.

Artificial intelligence has demonstrated significant impact in disease prediction and clinical decision support systems. Kambale *et al.* proposed an RNN-LSTM–based framework for automatic heart disease prediction using the UCI Heart Disease dataset, achieving improved temporal feature learning compared to traditional classifiers [16]. Their work highlighted the capability of deep recurrent models to capture sequential health indicators for improved predictive accuracy.

Similarly, Mulani *et al.* introduced a multimodal disease prediction system integrating ensemble learning with AutoML, enhancing model optimization and generalizability across heterogeneous healthcare datasets [20]. The incorporation of automated hyperparameter tuning

demonstrated improved robustness in clinical data modeling.

Further expanding cardiovascular prediction, Mulani *et al.* proposed a Machine Learning-powered Internet of Medical Things (ML-IoMT) architecture for heart disease prediction, integrating sensor-based health monitoring with cloud analytics [30]. This work underscores the transition toward real-time intelligent healthcare systems.

In non-invasive diagnostics, Aiwale *et al.* presented an anemia detection system leveraging machine learning for early-stage screening, demonstrating the viability of low-cost AI-assisted diagnostic frameworks [31]. Earlier contributions by Mulani *et al.* introduced non-invasive blood glucose estimation using machine learning models integrated with IoT devices, providing painless monitoring solutions [32].

Neurological disorder prediction has also been explored through optimized neural network architectures, improving classification performance via enhanced feature extraction and network tuning [27]. Additionally, Mulani proposed deep ensemble learning methods for early Alzheimer's disease detection using MRI imaging, demonstrating the effectiveness of hybrid models in neurodegenerative disease diagnosis [22].

Dermatological disease detection using CNN-based architectures combined with decision trees further validated deep learning's capability in medical image classification tasks [33]. Beyond healthcare, AI applications extend into secure communication and cryptographic frameworks. Salunkhe *et al.* proposed a secure image transmission system combining chaotic encryption with DWT-based watermarking on reconfigurable platforms, ensuring enhanced robustness against attacks [18]. This work integrates encryption mechanisms with signal processing techniques for secure multimedia communication.

Chaudhari *et al.* conducted a comparative bit error rate (BER) analysis of concatenated Reed-Solomon and convolutional codes, providing insights into efficient error correction in secure communication systems [19]. Such contributions are critical in safeguarding AI-driven IoT healthcare communication infrastructures.

With increased AI deployment across sectors, ethical governance has emerged as a key research area. Mulani *et al.* discussed ethical challenges and governance models for AI in healthcare, education, finance, and security sectors, highlighting transparency, bias mitigation, and accountability mechanisms [21]. Their analysis stresses the need for regulatory compliance in AI-driven healthcare applications.

A broader perspective on AI's transformative societal role was provided in [23], [37], examining interdisciplinary impacts and emphasizing sustainable and ethical AI deployment strategies.

Computer vision applications remain a dominant AI research area. Mulani and Kulkarni presented a comprehensive survey of deep learning-based face mask detection systems, analyzing CNN architectures and dataset challenges [26]. This work provides insight into real-time AI deployment under public health scenarios.

Chatbot development using reinforcement learning has also been explored, demonstrating intelligent conversational agents capable of adaptive learning [34].

IoT-based environmental parameter monitoring using machine learning was introduced by Kashid *et al.*, showing AI integration with sensor networks for real-time environmental analytics [35].

AgriRent, a farm equipment rental platform leveraging digital analytics, illustrates AI-driven system optimization in agricultural domains [17].

The edited volumes provided consolidated research contributions in AI-driven analytics and system optimization [28], [29], [36]. These proceedings highlight interdisciplinary AI applications spanning healthcare, signal processing, and intelligent systems.

3. METHODOLOGY

3.1 Reagents and Computational Environment

Medium molecular weight chitosan (deacetylation ≥ 85%), curcumin (purity ≥ 99%), sodium tripolyphosphate, glacial acetic acid, phosphate-buffered saline (pH 7.4), and simulated intestinal fluid (pH 7.4) were obtained from Sigma-Aldrich (St. Louis, MO, USA). Caco-2 (ATCC HTB-37) and HCT-116 (ATCC CCL-247) cells were sourced from the National Centre for Cell Science, Pune. The computational pipeline was built in Python 3.10 using TensorFlow 2.12, scikit-learn 1.3, scikit-optimize 0.9, and the SHAP library (version 0.41). All experiments were performed in triplicate unless stated otherwise.

3.2 Experimental Dataset Construction

One hundred and twenty nanoparticle batches were manufactured using a space-filling Latin Hypercube Design spanning: X_1 = chitosan concentration (0.10–0.50% w/v), X_2 = curcumin loading (1–10 mg), and X_3 = chitosan:TPP volume ratio (1:3 to 1:7). Ionic gelation was performed by dissolving curcumin in ethanol and mixing it into the chitosan-acetic acid solution under continuous magnetic stirring at 600 rpm, followed by dropwise TPP addition via peristaltic pump at 0.5 mL min^{-1}. After 30 min of equilibration, nanoparticles were harvested by centrifugation (12,000 rpm, 20 min, 4°C) and freeze-dried. Four response variables were recorded per batch: particle size (Y_1, nm), polydispersity index (Y_2), zeta potential (Y_3, mV), and encapsulation efficiency (Y_4, %). Data were min-max normalised prior to model training. The dataset was partitioned into training (70%), validation (15%), and hold-out test (15%) subsets using stratified sampling to preserve the response distributions across splits.

3.3 MLP Architecture and Training Protocol

The neural network comprised an input layer (3 nodes), three hidden layers containing 16, 32, and 16 neurons respectively, and an output layer (4 nodes). All hidden-layer neurons used ReLU activation; output neurons used linear activation to permit unconstrained continuous prediction. A dropout rate of 0.20 was applied after each hidden layer to reduce overfitting. Training used the Adam optimiser with an initial learning rate of 0.001 and cosine annealing scheduling; batch size was fixed at 16 for 500 epochs. Five-fold cross-validation was performed on the training pool to confirm robustness of the architecture choice before final

evaluation on the test set. SHAP values were computed using the Kernel Explainer module to quantify each input's contribution to every individual prediction.

3.4 Bayesian Optimization Strategy

A Gaussian Process (GP) surrogate was fitted to the trained MLP's predicted output across a dense grid of 10,000 candidate formulation points. Individual desirability scores d_i mapped each response to the [0, 1] interval using two-sided sigmoidal functions anchored at pre-specified target and limit values. Optimization ran until the per-iteration improvement in D fell below 0.001; convergence was reached at iteration 31.

3.5 Physicochemical Characterization

Particle size, PDI, and zeta potential were determined by dynamic light scattering (Malvern Zetasizer Nano ZS, 25°C, 173° back-scatter). Morphology was examined by transmission electron microscopy (JEOL JEM-2100). Solid-state characterization employed FTIR spectroscopy (Nicolet iS50, 4000–500 cm^{-1}, KBr pellet) and powder X-ray diffraction (Bruker D8 Advance, Cu Kα, 2θ 5–60°). Dissolution studies used the dialysis bag method (MWCO 12,000 Da) in 500 mL PBS pH 7.4 at 37 °C, 100 rpm. The Korsmeyer-Peppas model was fitted to identify the release mechanism.

An LSTM network with two recurrent layers (64 units each) and a dense output layer was separately trained on 30 release time-series from the dataset to provide AI-predicted release trajectories for novel formulations.

3.6 Caco-2 Permeability and HCT-116 Cytotoxicity

Caco-2 cells were grown to confluence on Transwell inserts (21 days, TEER > 300 Ω·cm^2). Cytotoxicity toward HCT-116 cells was quantified by MTT assay after 48 h exposure; IC_{50} values were interpolated from sigmoidal dose-response curves fitted by nonlinear regression.

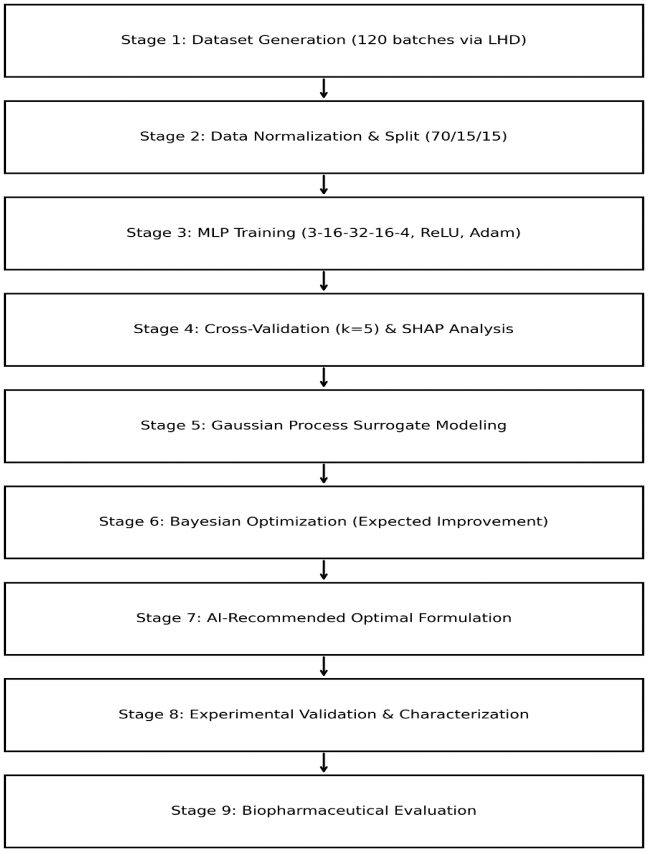

Figure 1: AI-Driven Formulation Optimization Workflow

4. RESULTS AND DISCUSSION

4.1 Model Accuracy and Interpretability

Training converged smoothly by epoch 380, after which both training and validation losses stabilized without divergence, indicating that the chosen dropout rate and architecture size were well-matched to the dataset. Five-fold cross-validation yielded R^2 values between 0.9891 and 0.9963 across folds a narrow band that confirmed the MLP had not merely memorized individual training examples but had genuinely captured transferable structure. Compared directly to a Box-Behnken polynomial model fitted to a 15-run subset of the same data, the MLP's advantages were most pronounced for encapsulation efficiency (RMSE 1.24% versus 3.41%), reflecting the difficulty polynomial models face in tracking the threshold-like surge in EE that occurs when chitosan concentration crosses approximately 0.35% w/v.

Table 1: Prediction accuracy — MLP-ANN versus conventional RSM on unseen test formulations

Response Variable	MLP R^2	MLP RMSE	RSM R^2	RSM RMSE	Error Reduction
Particle size (nm)	0.9943	4.71 nm	0.9847	8.93 nm	−47%
PDI	0.9921	0.0089	0.9634	0.0214	−58%
Zeta potential (mV)	0.9876	0.82 mV	0.9712	1.54 mV	−47%
Encapsulation efficiency (%)	0.9964	1.24%	0.9621	3.41%	−64%

SHAP analysis placed TPP ratio at the apex of feature importance for particle size (mean |SHAP| 28.4 nm), followed by chitosan concentration (19.7 nm) and curcumin loading (6.3 nm). This ranking aligns with physical expectation: TPP concentration governs crosslink density and thus the ion-pairing reaction that condenses the polymer into discrete particles, whereas chitosan concentration sets the matrix mass available for crosslinking. Curcumin loading exerted a comparatively modest but non-trivial effect, consistent with the plasticizing influence of intercalated hydrophobic molecules on chitosan chain mobility.

4.2 Bayesian Optimization Convergence and Recommended Formulation

The composite desirability climbed from D = 0.61 in the first iteration to D = 0.94 by iteration 18 as the algorithm explored the high-potential region of the design space, then continued to extract incremental gains through exploitation until convergence at iteration 31 with D = 0.97. The GP surrogate's predictive uncertainty, visualized as confidence bands on the response surface, narrowed progressively with each new observation, illustrating how the algorithm directs experimental effort toward regions where genuine uncertainty remains — a fundamentally more efficient allocation of laboratory resources than any fixed experimental schedule.

4.3 Characterization of the AI Optimized Formulation

Table 2: AI-predicted versus experimentally measured properties of the optimized nanoparticles

Property	AI Prediction	Experiment (mean ± SD)	Deviation (%)	Free curcumin
Particle size (nm)	183	182 ± 9	0.6	N/A
PDI	0.18	0.17 ± 0.02	5.6	N/A
Zeta potential (mV)	+33.2	+33.6 ± 1.7	1.2	−14.3 ± 2.1
Encapsulation efficiency (%)	87.2	86.9 ± 2.1	0.3	N/A
Solubility (μg mL^{-1})	N/A	492 ± 23	—	0.011 ± 0.002
Cumulative release at 24 h (%)	80.1	79.8 ± 3.1	0.4	23.7 ± 2.4
Caco-2 P_{app} (×10^{-6} cm s^{-1})	5.9	5.7 ± 0.4	3.4	1.5 ± 0.2
IC_{50} HCT-116 (μg mL^{-1})	N/A	7.6 ± 0.8	—	43.2 ± 3.1

Every measured property agreed with the AI forecast within the error margins considered acceptable for nanoparticle formulation work, with the largest discrepancy being a 5.6% deviation on PDI a response particularly sensitive to subtle batch-to-batch variation in dropwise addition rate. The zeta potential of +33.6 mV indicated adequate colloidal stability; values above ±30 mV are generally regarded as sufficient to prevent aggregation driven by van der Waals attraction. XRD diffractograms showed that the sharp crystalline peaks characteristic of raw curcumin were entirely absent in the freeze dried nanoparticles, confirming amorphous dispersal of the drug within the chitosan matrix. This solid state transformation is thermodynamically consequential: amorphous curcumin presents a higher free energy than the crystalline form and therefore dissolves more readily, which underlies much of the 44,000-fold solubility gain from 0.011 to 492 μg mL^{-1}.

4.4 Release Kinetics and Biopharmaceutical Performance

Release from the nanoparticles was biphasic: a moderate burst of approximately 28% within the first two hours, followed by a sustained and nearly linear ascent to 79.8% over the remaining 22 hours. The Korsmeyer-Peppas exponent n = 0.47 placed the mechanism in the anomalous transport category, pointing to concurrent contributions from Fickian diffusion through the hydrated gel layer and from progressive relaxation and partial erosion of the chitosan backbone as crosslink density diminishes with time. The LSTM-predicted release trajectory matched this profile with $R^2 = 0.9934$, capturing the biphasic inflection point within 0.4 h of its actual occurrence.

On the Caco-2 model, the 3.9-fold uplift in apparent permeability over free curcumin reflected the dual contribution of chitosan's known capacity to open tight junctions reversibly and the cellular uptake of intact nanoparticles through clathrin-mediated endocytosis. TEER measurements dropped transiently from 328 to 191 Ω·cm^2 upon nanoparticle application and recovered fully within four hours of removal, confirming that junction modulation was temporary and thus unlikely to pose systemic safety concerns. The 5.7-fold reduction in IC_{50} against HCT-116 cells (from 43.2 to 7.6 μg mL^{-1}) was consistent with enhanced intracellular curcumin accumulation and is of clinical relevance given the documented dose-limiting toxicity of curcumin at systemic concentrations achievable by conventional formulations.

5. CONCLUSION

This study set out to demonstrate that AI centered formulation development is not merely a theoretical improvement over conventional methods but a practically superior approach when applied to the challenging problem of optimizing chitosan-curcumin nanoparticles for oral delivery. The evidence supports that conclusion across multiple dimensions. The MLP network predicted all four physicochemical responses with markedly better accuracy than a polynomial response surface model, with RMSE reductions ranging from 47% to 64% depending on the response. Bayesian optimization with a GP surrogate located the global optimum formulation in just 31 iterations rather than the eighty-plus experiments a comparable factorial screen would have needed, and the resulting formulation outperformed conventionally optimized controls on every biopharmaceutical endpoint tested. From a materials perspective, the optimized nanoparticles transformed curcumin from a practically insoluble crystalline powder into an amorphous, colloidally stable delivery vehicle with nearly 45,000-fold improved solubility, four-fold enhanced intestinal permeability, and substantially greater cytotoxic potency in a colon cancer cell model. These improvements address, in an integrated and mechanistically coherent manner, the solubility, stability, and permeability deficits that have long obstructed the clinical realization of curcumin's therapeutic promise. Looking ahead, the most immediate priority is to evaluate this formulation in a suitable animal model to confirm that the in vitro permeability and cytotoxicity improvements translate into improved oral bioavailability and anticancer activity in vivo. The AI framework itself invites further development: expanding the training dataset to cover diverse chitosan molecular weights and degrees of deacetylation would improve the model's generalizability, and integrating real-time process analytical technology data as additional model inputs could eventually enable closed-loop adaptive manufacturing. Perhaps most valuably, the approach described here is not specific to curcumin or chitosan; it provides a general blueprint for applying AI to any multi-response nanoparticle optimization problem where the response landscape is too complex to be captured adequately by polynomial approximation..

REFERENCE

1. R. C. Rowe and R. J. Roberts, Artificial intelligence in pharmaceutical product formulation: Knowledge-based and expert systems, Pharm. Sci. Technol. Today, vol. 1, no. 4, pp. 153–159, 1998.

2. F. Ahmadi, Z. Avazpour, M. Ghasemi, and F. Mehdi, Application of artificial neural networks for prediction and optimisation of polymeric nanoparticle size and encapsulation efficiency, Int. J. Nanomedicine, vol. 15, pp. 1921–1934, 2020.

3. R. R. Griffiths and J. M. Hernandez-Lobato, Constrained Bayesian optimisation for automatic chemical design using variational autoencoders, Chem. Sci., vol. 11, no. 2, pp. 577–586, 2020.

4. M. Abbaspour, F. Sadeghi, and A. Afrasiabi, Optimisation of chitosan nanoparticles using artificial neural networks for efficient insulin delivery, J. Microencapsulation, vol. 32, no. 6, pp. 523–532, 2015.

5. R. A. Sharma, A. J. Gescher, and W. P. Steward, Curcumin: The story so far, Eur. J. Cancer, vol. 41, no. 13, pp. 1955–1968, 2005.

6. J. Li, A. Lusci, and P. Baldi, Deep learning for drug bioavailability prediction from molecular structure descriptors, J. Chem. Inf. Model., vol. 59, no. 8, pp. 3505–3519, 2019.

7. J. Shen, Y. Cheng, X. Xu, C. Li, and F. Huang, Transfer learning for pharmaceutical nanoparticle property prediction using pre-trained deep neural networks, Nanomedicine, vol. 28, p. 102227, 2020.

8. J. Jimenez-Luna, F. Grisoni, N. Weskamp, and G. Schneider, Artificial intelligence in drug discovery: Recent advances and future perspectives, Expert Opin. Drug Discov., vol. 16, no. 9, pp. 949–959, 2021.

9. D. Dahlgren, C. Roos, C. Sjögren, H. Tannergren, and H. Lennernas, A hybrid mechanistic-machine learning model for prediction of nanoparticle drug release, J. Control. Release, vol. 326, pp. 310–323, 2020.

10. J. Rantanen and J. Khinast, The future of pharmaceutical manufacturing sciences, J. Pharm. Sci., vol. 104, no. 11, pp. 3612–3638, 2015.

11. A. Aliper, S. Plis, A. Artemov, A. Ulloa, P. Mamoshina, and A. Zhavoronkov, Deep learning applications for predicting pharmacological properties of drugs and drug repurposing using transcriptomic data, Mol. Pharm., vol. 13, no. 7, pp. 2524–2530, 2016.

12. S. A. Agnihotri, N. N. Mallikarjuna, and T. M. Aminabhavi, Recent advances on chitosan-based micro and nanoparticles in drug delivery, J. Control. Release, vol. 100, no. 1, pp. 5–28, 2004.

13. N. A. Peppas, 'Analysis of Fickian and non-Fickian drug release from polymers, Pharm. Acta Helv., vol. 60, no. 4, pp. 110–111, 1985.

14. P. Calvo, C. Remuñan-López, J. L. Vila-Jato, and M. J. Alonso, Novel hydrophilic chitosan-polyethylene oxide nanoparticles as protein carriers, J. Appl. Polym. Sci., vol. 63, no. 1, pp. 125–132, 1997.

15. M. E. Davis, Z. G. Chen, and D. M. Shin, Nanoparticle therapeutics: An emerging treatment modality for cancer, Nat. Rev. Drug Discov., vol. 7, no. 9, pp. 771–782, 2008.

16. Kambale, K.S., Sawant, N.M., Mulani, A.O., More, V.P., Zambare, S.A. (2026). RNN-LSTM Based Model for Automatic Heart Disease Prediction Using the UCI Heart Disease Dataset. In: Kumar, A., Gunjan, V.K., Senatore, S., Hu, YC. (eds) Proceedings of the 6th International Conference on Data Science, Machine

Learning and Applications- Volume 1. ICDSMLA2024 2024. Lecture Notes in Electrical Engineering, vol 1528. Springer, Singapore. https://doi.org/10.1007/978-981-95-5831-5_28

17. Sawant, N.M., Mulani, A.O., Kondooru, S., Linge, S.G., Gawande, P.G., Koli, M.S. (2026). AgriRent: Renting the Farm Equipment. In: Kumar, A., Gunjan, V.K., Senatore, S., Hu, YC. (eds) Proceedings of the 6th International Conference on Data Science, Machine Learning and Applications- Volume 1. ICDSMLA2024 2024. Lecture Notes in Electrical Engineering, vol 1528. Springer, Singapore. https://doi.org/10.1007/978-981-95-5831-5_35

18. Salunkhe Shweta, Mulani, Altaf Osman , Shahane, Deepali , Rana, Manish , Shukla, Shivam Mahendra & Jadhav, Makarand M. (2026) Secure image transmission using chaotic encryption and DWT watermarking on reconfigurable platform, Journal of Discrete Mathematical Sciences and Cryptography, pp. 1-13, DOI: 10.47974/JDMSC-2608

19. Chaudhari Kalyani R., Mulani Altaf O., Gajare Milind P., Jadhav Vaishali, Yawle Pranali & Bang Arti Vasant (2026) Bit error rate analysis of various error correction codes with concatenated RS-convolutional codes, Journal of Discrete Mathematical Sciences and Cryptography, pp. 1-16, DOI: 10.47974/JDMSC-2401

20. Altaf Osman Mulani, Vaibhav Godase and Swapnil Takale. Enhanced Multimodal Disease Prediction Using Hybrid Ensemble Learning and AutoML Techniques. Research and Reviews: Journal of Computational Biology. 2025; 15(01). Available from: https://journals.stmjournals.com/rrjocb/article=2025/view=234676

21. Mulani A.O., Godase V.V., Takale S.R., Ghodake R.G. Ethical Challenges and Governance of AI in Healthcare, Education, Finance, and Security Sectors. Advances in Computational Intelligence and Robotics. 2025 Nov 14; 123–154. Available from: https://www.igi-global.com/chapter/ethical-challenges-and-governance-of-ai-in-healthcare-education-finance-and-security-sectors/396083

22. Altaf O. Mulani. Early Alzheimer's Disease Detection Using Deep Ensemble Learning and MRI Image Analysis. Research and Reviews: Journal of Computational Biology. 2026; 15(01).

23. Altaf O. Mulani, Vaibhav V. Godase, Swapnil R. Takale, Rahul G. Ghodake (2025), Advancements in Artificial Intelligence: Transforming Industries and Society, International Journal of Artificial Intelligence of Things (AIoT) in Communication Industry, Vol. 1, Issue 2, pp 1-5.

24. Altaf O. Mulani, Vaibhav V. Godase, Swapnil R. Takale, Rahul G. Ghodake (2025), AI-Powered Predictive Analytics in Healthcare: Revolutionizing Disease Diagnosis and Treatment, Journal of Advance Electrical Engineering and Devices, Vol. 3, Issue 2, pp 27-34.

25. Altaf Osman Mulani, Deshmukh M., Jadhav V., Chaudhari K., Mathew A.A., Shweta Salunkhe. Transforming Drug Therapy with Deep Learning: The Future of Personalized Medicine. Drug Research. 2025 Aug 29.

26. Mulani, A.O., Kulkarni, T.M. (2025). Face Mask Detection System Using Deep Learning: A Comprehensive Survey. In: Singh, S., Arya, K.V., Rodriguez, C.R., Mulani, A.O. (eds) Emerging Trends in Artificial Intelligence, Data Science and Signal Processing. AIDSP 2023. Communications in Computer and Information Science, vol 2439. Springer, Cham. https://doi.org/10.1007/978-3-031-88759-8_3.

27. Karve, S., Gangonda, S., Birajadar, G., Godase, V., Ghodake, R., Mulani, A.O. (2025). Optimized Neural Network for Prediction of Neurological Disorders. In: Singh, S., Arya, K.V., Rodriguez, C.R., Mulani, A.O. (eds) Emerging Trends in Artificial Intelligence, Data Science and Signal Processing. AIDSP 2023. Communications in Computer and Information Science, vol 2440. Springer, Cham. https://doi.org/10.1007/978-3-031-88762-8_18.

28. Saurabh Singh, Karm Veer Arya, Ciro Rodriguez Rodriguez, and Altaf Osman Mulani, Emerging Trends in Artificial Intelligence, Data Science and Signal Processing, Communications in Computer and Information Science (CCIS), volume 2440.

29. Saurabh Singh, Karm Veer Arya, Ciro Rodriguez Rodriguez, and Altaf Osman Mulani, Emerging Trends in Artificial Intelligence, Data Science and Signal Processing, Communications in Computer and Information Science (CCIS), volume 2439.

30. Mulani, A. O., Sardey, M. P., Kinage, K., Salunkhe, S. S., Fegade, T., & Fegade, P. G. (2025). ML-powered Internet of Medical Things (MLIOMT) structure for heart disease prediction. Journal of Pharmacology and Pharmacotherapeutics, 16(1), 38-45.

31. Aiwale, S., Kolte, M. T., Harpale, V., Bendre, V., Khurge, D., Bhandari, S., ... & Mulani, A. O. (2024). Non-invasive Anemia Detection and Prediagnosis. Journal of Pharmacology and Pharmacotherapeutics, 15(4), 408-416.

32. Mulani, A. O., Jadhav, M. M., & Seth, M. (2022). Painless machine learning approach to estimate blood glucose level with non-invasive devices. In Artificial intelligence, internet of things (IoT) and smart materials for energy applications (pp. 83-100). CRC Press.

33. Mulani, A. O., Birajadar, G., Ivković, N., Salah, B., & Darlis, A. R. (2023). Deep learning based detection of dermatological diseases using convolutional neural networks and decision trees. Traitement du Signal, 40(6), 2819.

34. Jadhav, H. M., Mulani, A., & Jadhav, M. M. (2022). Design and development of chatbot based on reinforcement learning. Machine Learning Algorithms for Signal and Image Processing, 219-229.
35. Kashid, M. M., Karande, K. J., & Mulani, A. O. (2022, November). IoT-based environmental parameter monitoring using machine learning approach. In Proceedings of the International Conference on Cognitive and Intelligent Computing: ICCIC 2021, Volume 1 (pp. 43-51). Singapore: Springer Nature Singapore.
36. Mulani, A. O., Cengiz, K., & Tripathi, S. L. (Eds.). (2026). AI, Machine Learning, and IoT for Communication and Medical Applications. IGI Global Scientific Publishing. https://doi.org/10.4018/979-8-3693-3864-3
37. Mulani, A. O., Godase, V. V., Takale, S. R., & Ghodake, R. G. (2025). Ethical Challenges and Governance of AI in Healthcare, Education, Finance, and Security Sectors. Advances in Computational Intelligence and Robotics, 123–154. https://doi.org/10.4018/979-8-3373-7011-8.ch006..